The Journal of the Korean Society of
Coastal and Ocean Engineers
Vol. 6, No. 2, pp. 157~163, June 1994

An Experimental Study on Wave Energy Variation through Breaking Processes
碎破過程에서의 波浪에너지 變化에 관한 實驗硏究

Won Chul Cho*
조 원 철*

Abstract □ An experimental study of deep-water breaking waves is performed by nonlinear wave evolution as well as superposition of different wave frequencies. Two-dimensional and three-dimensional wave instabilities and breakings are observed in nonlinear wave evolution. The wave energy evolves with almost the same initial wave energy before breaking but decreases significantly after breaking process. Large spilling and plunging waves are generated near the expected breaking location by means of faster waves overtaking slow waves at a certain point. More energy loss in vigorous plunging breakers is observed through breaking process.

要 旨 : 비선형 심해파의 전개과정을 통하여 그리고 어떤 특정한 위치에서 파속이 빠른 파가 느린 파를 추월하도록 하여 파의 중복을 유도함으로써 심해쇄파를 발생시키는 실험을 수행하였다. 2차원과 3차원적인 파랑의 불안정상태와 그로 인한 쇄파의 발생이 비선형 심해파의 전개과정에서 관찰되었고 또한 예상 쇄파지점에서 큰 파고를 갖는 崩壞波(spilling waves)와 卷波(plunging waves)를 관찰하였다. 비선형 심해파의 전개에서는 파랑이 거의 초기에너지를 가지고 전개하였으며 쇄파가 일어난 후에는 많은 에너지가 감소하는 것으로 나타났다. 崩壞波와 卷波에서도 쇄파후의 에너지의 감소가 나타났지만 특히 격렬한 卷波에서의 에너지감소가 두드러지게 관찰되었다.

1. INTRODUCTION

Breaking waves in deep water are important in many areas of ocean science and technology. Wave breaking plays a crucial role in the transfer of energy from the wave field to wind-generated surface currents. It also generates intensive turbulence within the underlying flow field, which mixes the upper layer of the ocean and enhances the transfer of heat and momentum across the air-sea interface.

During the past two decades, many studies have been conducted to understand the breaking process in the wave evolution. Benjamin and Feir (1967) discovered that a uniform deep-water wave train with constant wave frequency becomes highly irregular and unstable and finally breaks far from its origin due to modulational perturbations of side-band frequency components. Melville (1982) investigated uniform deep-water wave instability and breaking and observed two-dimensional Benjamin-Feir instability at the wave steepness less than 0.31 as well as three-dimensional instability at the wave steepness larger than 0.31. He also found at the initial stage of the wave evolution, the upper and the lower side-band frequencies were developed asymmetrically about the fundamental frequency and its higher harmonics (the upper side-band frequency being larger than the lower side-band frequency). However, at the onset of breaking, the lower side-band frequency grew rapidly and became dominant in the wave field after breaking. Su *et al.* (1982) carried out an experimental work and also observed two- and three-dimensional instabilities and large growth of the lower side-band frequency after brea-

*한국해양연구소 해양공학연구부 (Ocean Engineering Division, Korea Ocean Research and Development Institute, P.O. Box 29 Ansan 425-600, Korea)

king.

On the other hand, Longuet-Higgins (1974) developed a method, 'Storm Building', to generate breaking waves in the laboratory, which requires the generation of waves with decreasing wave frequency, so that faster waves overtake slow waves at some distance away from the wave paddle, summing up to produce a steep and unstable wave. Kjeldsen and Myrhaug (1979) analyzed extremely unstable waves just before breaking using the zero-downcross method. They found that the crest front steepness (the crest elevation above mean water level/the horizontal distance from the zero-upcross to the wave crest) was the most important factor in deciding the type of breaking wave, and breaking occurred in the range of front wave steepness between 0.32 and 0.78 (the highest value for a plunging breaker). Ducan *et al.* (1987) also analyzed breaking waves using the crest front steepness, and found that the crest front steepness increased slowly up to the breaking point and then decreased during the beginning of the breaking process with the average value of 0.5 for a spilling breaker and 0.7 for a plunging breaker.

Most laboratory studies on wave instability and breaking of deep-water wave train have been based on Benjamin and Feir's wave instability and Longuet-Higgins wave breaking. In the present study, wave instability and breaking are also investigated by constant wave frequency with various wave amplitudes and by stong wave-wave interaction.

2. THEORY

2.1 Breaking Wave Generation through the Instability of a Nonlinear Deep-Water Wave

A theoretical analysis of wave instability was presented by Benjamin and Feir (1967), who showed that a uniform continuous wave train with fundamental wave frequency, ω, is unstable to infinitesimal perturbations in side-band frequencies, $\omega(1\pm\delta)$, when δ is in the range between 0 and $\sqrt{2}\,ka$ (where δ is a small perturbation in wave frequency of the order (ka), k is the wave number and a is the perturbed wave amplitude). They derived Eq. (2) for the perturbed free-surface elevation, $\eta(x,t)+\varepsilon(x,t)$, which is corresponding to a nearly uniform wave train with a weak amplitude modulation, from the surface elevation, Eq. (1), which includes the first two harmonics.

$$\eta(x,t)=a\cos(kx-\omega t)+\frac{1}{2}ka^2\cos 2(kx-\omega t) \tag{1}$$

$$\eta_p(x,t)=a\cos(kx-\omega t)+\varepsilon_+\cos[k(1+\kappa)x-\omega(1+\delta)t]+\varepsilon_-\cos[k(1-\kappa)x-\omega(1-\delta)t] \tag{2}$$

where κ and δ are the small perturbations in wave number and frequency, respectively. $\varepsilon_{+,-}=\exp[1/2\delta(2k^2a^2-\delta^2)^{1/2}\omega t]$ represents the amplitude of the side-band disturbances. $\eta_p(x,t)$ displays a gradual modulation of the fundamental waveform, $a\cos(kx-\omega t)$. For a given value of the wave steepness, ka, of the initial wave, the unstable side-band amplitudes grow exponentially with time if $0<\delta\leq\sqrt{2}ka$, with the growth rate having a maximum value at $\delta=ka$.

2.2 Breaking Wave Generation through Transient Wave Convergence

It was shown by Longuet-Higgins (1974) that wave trains with decreasing frequencies converge at a single point in time and space. The method he developed is described in Cho and Bruno (1992).

3. EXPERIMENT

Experiments were performed at Davidson Laboratory of Stevens Institute of Technology in Hoboken, New Jersey, U.S.A., where the wave channel is 313 feet long, 12 feet wide, and the water depth is 5.4 feet. The fresh water is filled in the wave channel and continuously filtered. The side walls of the wave channel are concrete, with no opening to observe the water column outside the tank and a wave absorbing beach at the other. The dual flap is composed of lower flap and upper flap in which the lower flap is hinged on the channel floor and the upper flap is hinged on the top of the lower flap. The wavemaker is controlled by PDP-11 microcomputer which calculates the digital signal form of the flap motion as a function of time for a given wave frequency and height. These time series are converted to control voltage corresponding to the

stored digital sequence at a predetermined time interval through the digital-to-analog converter. Then, the hydraulic servo system produces a specific wave form proportional to the applied sinusoidal flap angles.

The wooden sloping beach at the end opposite the wavemaker dissipates propagating waves and absorbs incident wave energy to minimize wave reflection during tests. Owing to the relatively long wave channel and the short duration of each test within 1 minute, waves were not disturbed by reflection from the beach, which may yield slow modulations to incident waves.

Evolution of the surface wave train for wave instability and breaking was measured as waves propagated down the channel, using 5 wave gauges located at 20, 70, 120, 170, and 220 ft from the wavemaker. Six wave gauges were used for the measurement of spilling and plunging breaking waves. These gauges were installed at 20, 45, 70, 95, 120, and 145 ft from the wavemaker for breaking waves occurred at 102 ft. Wave gauges were calibrated daily using vertical traverse mechanisms mounted above the water surface in the wave channel. There was only negligible difference in each calibration.

The data acquisition program digitizes analog signals from the instruments by an analog-to-digital converter at a selected rate, and records them on the disk in digital form as the test progresses. The spectral analysis program, which contains Blackman-Tukey auto-correlation procedure, calculates power spectral density of the signal recorded in a time history file.

4. RESULTS

4.1 Evolution of Nonlinear Wave Train

At the wave steepness of 0.204 (f=1.0 Hz and a=2 inches), two-dimensional Benjamin-Feir instability and breaking occurred downstream, with slowly developing wave amplitude modulations before breaking location. The breaking profile was nearly uniform across the channel (Fig. 1).

The lower side-band frequency grows from the initial stage and then the upper side-band frequency follows with very small magnitude. The upper and

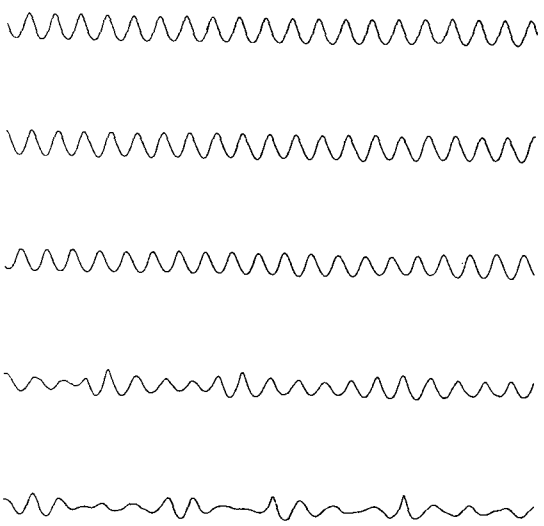

Fig. 1. Wave profiles of ka=0.204. Measuring stations at 20, 70, 120, 170, and 220 ft from the wavemaker.

lower side-band frequencies around f_{upp}=1.204 Hz and f_{low}=0.796 Hz become symmetric in the middle of evolution (x=120 ft in Fig. 2), but as the lower side-band frequency develops rapidly downstream, the symmetric form between the upper and the lower side-band frequencies does not appear any more. The fundamental wave frequency is dominant in the wave field through the wave evolution (Fig. 2).

As the wave steepness is increased to 0.307 (f=1.0 Hz and a=3 inches), three-dimensional wave instability was developed upstream as the result of transverse perturbations cross the wave channel. As the wave train evolved midstream, the wave train was transformed in its shape and became vertically asymmetric with increasing slope of the front face and deepening of the trough, so that ultimately three-dimensional breaking occurred with a couple of localized breaking waves in a row. After three-dimensional breaking process, new two-dimensional second breaking occurred with weak breaking intensity. A series of two-dimensional wave groups was observed after the second breaking, with significantly decreasing wave steepness and propagating wave energy (Fig. 3).

Unlike the frequency modulation of the two-dimensional instab[illegible] ka=0.204, the magnitude

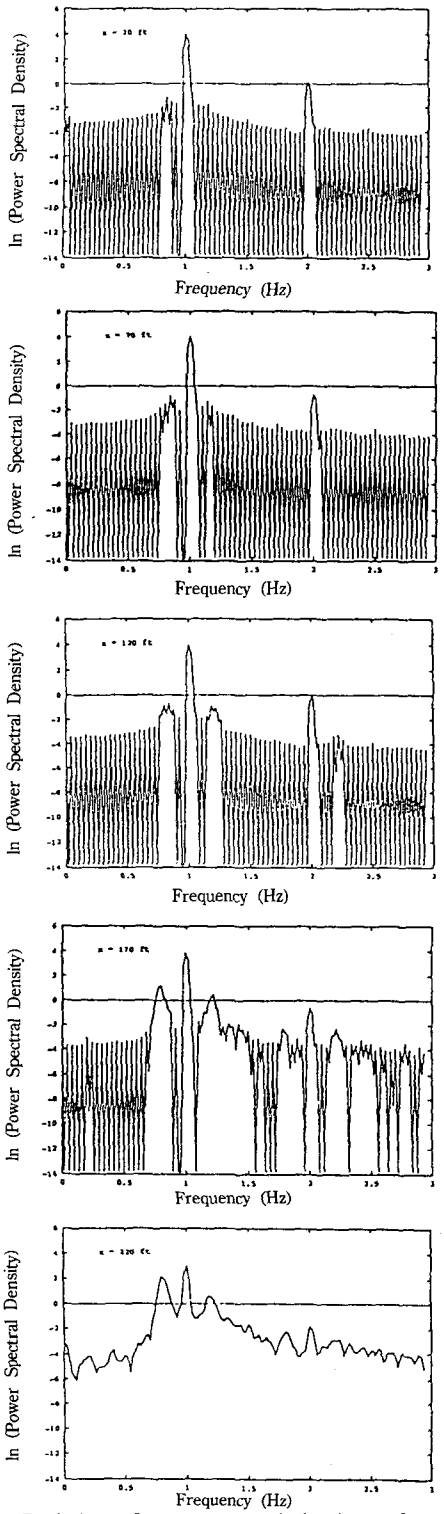

Fig. 2. Evolution of power spectral density at $ka=0.204$. Power spectral density=(in[illegible]. Breaking between x=170 and 220 ft.

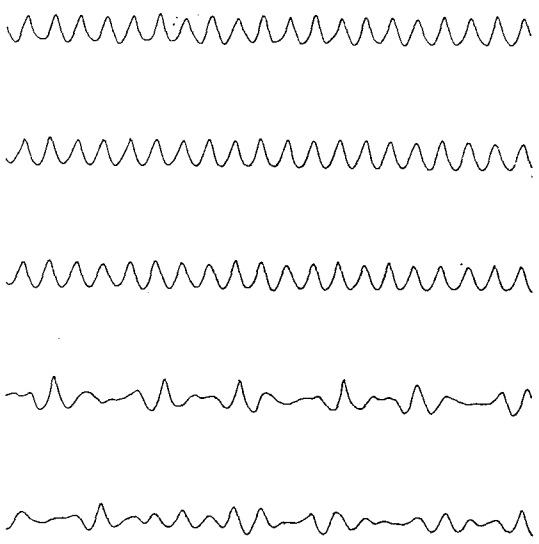

Fig. 3. Wave profiles of $ka=0.307$. Measuring stations at 20, 70, 120, 170, and 220 ft from the wavemaker.

of the upper side-band frequency around $f_{upp}=1.307$ Hz is developed first at the inital stage and then the lower side-band frequency around $f_{low}=0.693$ Hz begins to grow further down the channel with slightly larger magnitude than that of the upper side-band frequency, showing asymmetric development. The lower side-band frequency grows rapidly as the wave train evolves downstream, while the upper side-band frequency remains constant or diminishes (Fig. 4).

At the wave steepness, $ka=0.409$ ($f=1.0$ Hz and $a=4$ inches), frequent, short, and small three-dimensional top-crest breaking has different breaking properties than three-dimensional breaking and seems to be the result of the superharmonic instability(Longuet-Higgins, 1978a), which has the same or less horizontal perturbation scale as the fundamental wavelength. As wave train approached midstream, top-crest breaking deformed to longer three-dimensional breaking due to the subharmonic perturbaton (Longuet-Higgins, 1978b), which has a greater horizontal perturbation scale than the fundamental wavelength. After the first breaking, even though there existed weak three-dimensional wave instability in the wave train, weak two-dimensional second breaking occurred downstream (Fig. 5).

The fundamental wave frequency dominates the

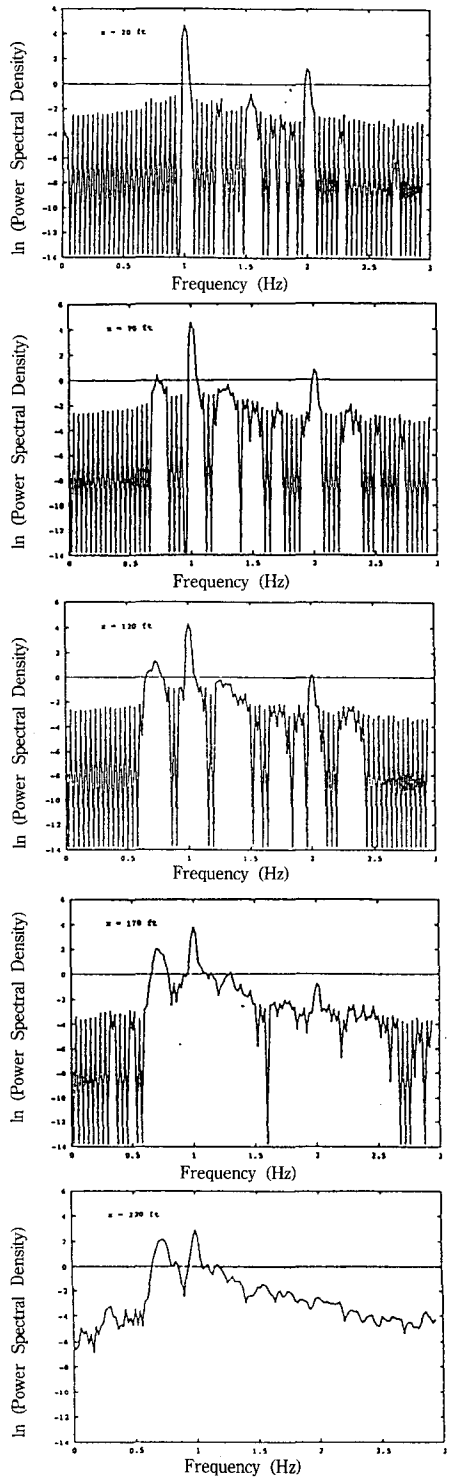

ɟ. 4. Evolution of power spectral density at $ka=0.307$. Power spectral density=(in)²/Hz. Breaking between x=120 and 170 ft (1st), and x=170 and 220 ft (2nd).

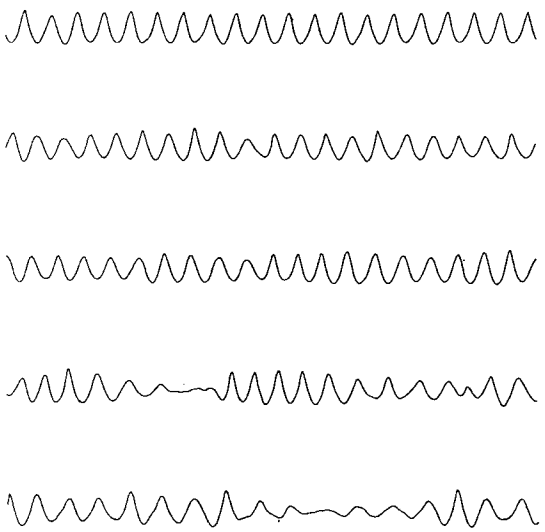

Fig. 5. Wave profiles of $ka=0.409$. Measuring stations at 20, 70, 120, 170, and 220 ft from the wavemaker.

wave field at the early stage in spite of frequent top-crest breaking with strong three-dimensional instability. However, due to the effect of the superharmonic perturbation, very small growth of the upper side-band frequency is developed at the initial stage at $f_{upp}=1.5$ Hz. Very small magnitude of lower side-band frequency is also observed upstream after the upper side-band frequency appeared and shows symmetric form with the upper side-band frequency. The magnitude of the fundamental wave frequency diminishes with large decreasing rate as the wave train gets through the superharmonic perturbation, while the lower side-band wave frequency grows rapidly as subharmonic perturbation is developed. The lower side-band frequency at $f_{low}=0.81$ becomes the dominatnt wave frequency at the final stage after the second breaking process (Fig. 6).

Dimensionless wave energy variation, which is obtained by normalizing the wave energy at each measuring station, E, with respect to the wave energy at reference measuring station, E_o, is displayed in Fig. 7. The x-axis is the normalized measuring station by the length of the wave channel, X_{wc}. In two-dimensional wave instability at $ka=0.204$, wave energy evolves with almost the same initial wave energy up to downstream before breaking. As wave approaches the br ng location wave energy inc-

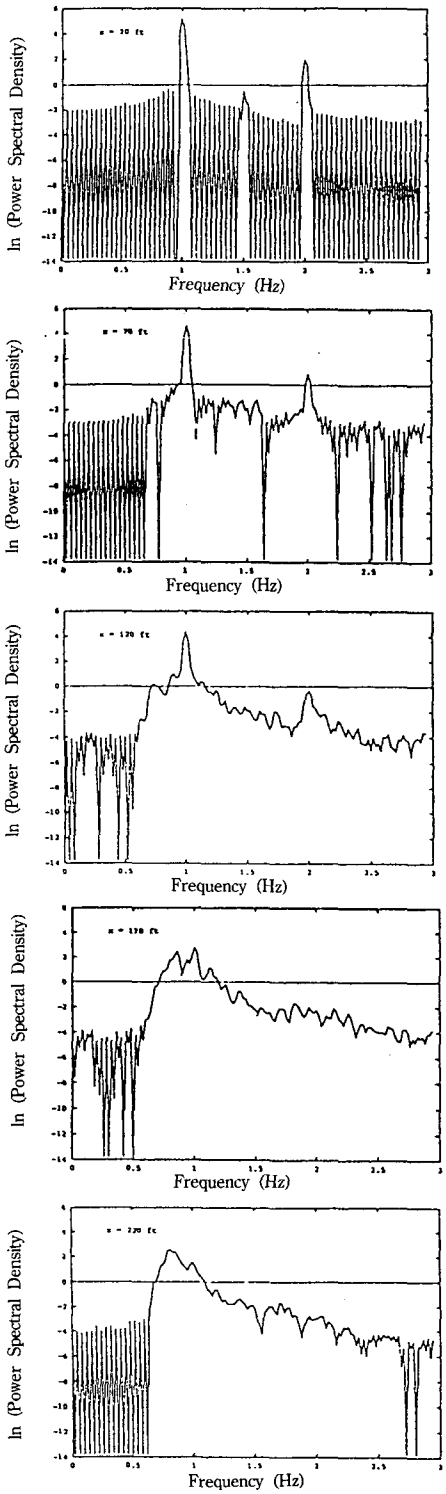

Fig. 6. Evolution of power spectral density at ka=0.409. Power spectral density=(in)^2/Hz. Breaking between z=70 and 120 ft (1st), and x= 170 and 220 ft (2nd)

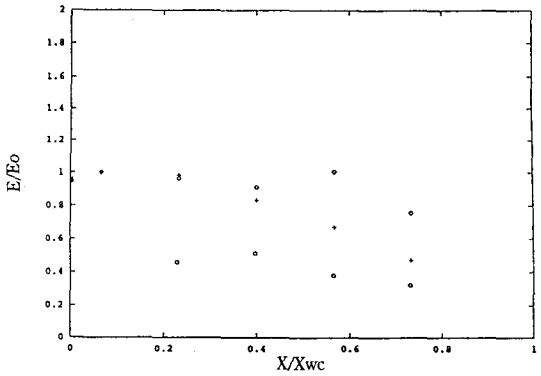

Fig. 7. Wave energy variation at ka=0.204 (◇), ka=0.307 (+) and ka=0.409 (○).

reases with a small rate with the wave front face becoming steeper and with slightly increasing wave amplitude, and then decreases after breaking process. At the wave steepness of 0.307, wave energy is decreased slightly through three-dimensional breaking preocesses of conversing of the outwardly-dissipating wave energy and inwardly-reflecting wave energy by the effects of side walls of the wave channel, and decreased significantly after the first three-demensional breaking and the second two-dimensional breaking processes occurring in the center and at the sides of the wave channel due to the slowly decaying three-dimensional instability effects. Due to top-crest breaking and superharmonic upstream, at the wave steepness of 0.409, wave energy decreased abruptly from the early stage. Wave energy grows with a small rate in the three-dimensional breaking region with relatively longer wave length and decreases again after three-dimensional breaking and two-dimensional second breaking downstream. Therefore, it is inferred that wave energy reduces its magnitude through breaking process as well as friction effect on the wall of the wave channel.

4.2 Evolution of Large Breaking Wave

A wave group, short wave followed by long wave with linearly increasing wave amplitude and constant wave frequency decrement rate, was generated for large spilling and plunging breaking wave tests. As the wave envelop propagated down the wave channel, the wave train was greatly modulated in its shape, with decreasing wave length and period,

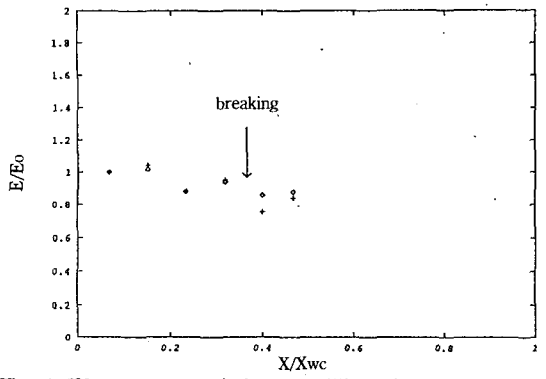

Fig. 8. Wave energy variation in spilling (◇) and plunging (+) breaking waves. Wave group parameters of f=0.76−0.585 Hz, df=0.025 Hz, X_b=102 ft, and $(ka)_{ave}$=0.17 for spilling and 0.178 for plunging.

and reached a maximum steepness near the predicted breaking location and then dispersed downstream after breaking. The type of breaking wave, spilling or plunging, was decided by initial wave amplitude and wave frequency range, which are the main factors of initial wave steepness. The results of large breaking wave tests have been presented in Cho and Bruno (1992).

The wave energy variation for spilling and plunging breakers along the wave channel is shown in Fig. 8. The energy in spilling and plunging breakers develops with nearly same shape, oscillating its magnitude before breaking, however, at near the breaking point, energy in both cases increases as wave elevation reaches at critical point. After breaking, one distinct phenomenon is shown that the energy at plunging breaking wave is decreased more than that of the spilling breaking wave due to more loss of energy from severe breaking process. Wave energy grows slightly after breaking region in both cases.

5. CONCLUSION

Various deep-water breaking wave tests were performed to investigate Benjamin-Feir wave instability and Longuet-Higgins large breaking waves. Two-dimensional and three-dimensional wave instabilities and breakings were observed from nonlinear deep-water wave train evolution. Large spilling and plunging breaking waves were generated by strong wave-wave interaction, as faster waves with higher wave frequencies overtook short waves with low wave frequencies at a certain location in time.

The experimental results show that for the small wave steepness, ka=0.204, a uniform deep-water wave train undergoes two-dimensional Benjamin-Feir instability and ultimately leads to breaking. Three-dimensional wave instability and breaking is shown at ka=0.307. At the wave steepness of 0.409, three-dimensional instability with top-crest breaking evolves at the early stage as transverse perturbations grow rapidly across the channel. As the wave train propagates midstream, top-crest breaking is transformed to the relatively longer localized three-dimensional breaking with subharmonic structure.

Two-dimensional second breaking is also developed downstream with significantly decreased wave steepness. These top-crest and three-dimensional breakers resemble real breaking in the open ocean.

Wave energy in nonlinear wave evolution evolves with the almost same initial wave energy before breaking but drops its magnitude after breaking process. The loss of wave energy in the plunging breaking event is greater than that in the spilling breaking, and wave energy recovers slightly after the breaking region.

REFERENCES

Benjamin, T.B. and Feir, J.E., 1967. The disintegration of wave trains in deep water, Part 1. Theory, *J. Fluid Mech.*, **27**: 417-430.

Duncan, J.H., Wallendorf, L.A. and Johnson, B., 1987. An experimental investigation of the kinematic of breaking waves, Report No. EW-7-87, U.S. Naval Academy.

Kjeldsen, S.P. and Myrhaug, D., 1979. Breaking waves in deep water and resulting wave forces, *Proc. 11th offshore Technology Conf. Houston*, Texas, Paper No. 3646.

Longuet-Higgins, M.S., 1974. Breaking waves in deep or shallow water, *Proc 10th Conf. on Naval Hydrodynamics*, 597-605.

Longuet-Higgins, M.S., 1978a. The instability of gravity wave of infinite amplitude in deep water. I. superharmonics, *Proc. R. Soc. Lond.*, **A360**, 471-488.

Longuet-Higgins, M.S., 1987b. The instability of gravity waves of infinite amplitude in deep water. II. Subharmonics, *Proc. R. Soc. Lond.*, **A360**, 489-505.

Melville, W.K., 1982. The instability and breaking of deep-water waves, *J. Fluid Mech.*, **115**: 165-185.

Su, M., Bergin, M., Marler, P. and Myrick, R., 1982. Experiments on nonlinear instabilities and evolution of steep gravity-wave train, *J. Fluid Mech.*, **124**: 46-72.

Cho, W.C. and Bruno, M., 1992. Breaking wave generation in the laboratory, *J. Korean Society of Coastal and Ocean Engineers*, **4**(3): 178-186.